Mechanisms of UV-B light-induced photoreceptor UVR8 nuclear localization dynamics

Fang Fang[1]* (iD), **Li Lin**[1,2,3]* (iD), **Qianwen Zhang**[1]* (iD), **Min Lu**[4], **Mariya Y. Skvortsova**[5], **Roman Podolec**[5,6] (iD), **Qinyun Zhang**[1] (iD), **Jiahao Pi**[1] (iD), **Chunli Zhang**[1] (iD), **Roman Ulm**[5,6] (iD) and **Ruohe Yin**[1,2,3] (iD)

[1]School of Agriculture and Biology, Shanghai Jiao Tong University, 800 Dongchuan Road, Minhang District, Shanghai 200240, China; [2]Key Laboratory of Urban Agriculture Ministry of Agriculture, Shanghai Jiao Tong University, Shanghai 200240, China; [3]Joint Center for Single Cell Biology, Shanghai Jiao Tong University, Shanghai 200240, China; [4]Department of Orthopaedics, Shanghai Key Laboratory for Prevention and Treatment of Bone and Joint Diseases, Shanghai Institute of Traumatology and Orthopaedics, Ruijin Hospital, Shanghai Jiao Tong University School of Medicine, Shanghai 200025, China; [5]Department of Botany and Plant Biology, Section of Biology, Faculty of Sciences, University of Geneva, CH-1211 Geneva 4, Switzerland; [6]Institute of Genetics and Genomics of Geneva (iGE3), University of Geneva, CH-1211 Geneva 4, Switzerland

Summary

• Light regulates the subcellular localization of plant photoreceptors, a key step in light signaling. Ultraviolet-B radiation (UV-B) induces the plant photoreceptor UV RESISTANCE LOCUS 8 (UVR8) nuclear accumulation, where it regulates photomorphogenesis. However, the molecular mechanism for the UV-B-regulated UVR8 nuclear localization dynamics is unknown.

• With fluorescence recovery after photobleaching (FRAP), cell fractionation followed by immunoblotting and co-immunoprecipitation (Co-IP) assays we tested the function of UVR8-interacting proteins including CONSTITUTIVELY PHOTOMORPHOGENIC 1 (COP1), REPRESSOR OF UV-B PHOTOMORPHOGENESIS 1 (RUP1) and RUP2 in the regulation of UVR8 nuclear dynamics in *Arabidopsis thaliana*.

• We showed that UV-B-induced rapid UVR8 nuclear translocation is independent of COP1, which previously was shown to be required for UV-B-induced UVR8 nuclear accumulation. Instead, we provide evidence that the UV-B-induced UVR8 homodimer-to-monomer photoswitch and the concurrent size reduction of UVR8 enables its monomer nuclear translocation, most likely via free diffusion. Nuclear COP1 interacts with UV-B-activated UVR8 monomer, thereby promoting UVR8 nuclear retention. Conversely, RUP1 and RUP2, whose expressions are induced by UV-B, inhibit UVR8 nuclear retention via attenuating the UVR8–COP1 interaction, allowing UVR8 to exit the nucleus.

• Collectively, our data suggest that UV-B-induced monomerization of UVR8 promotes its nuclear translocation via free diffusion. In the nucleus, COP1 binding promotes UVR8 monomer nuclear retention, which is counterbalanced by the major negative regulators RUP1 and RUP2.

Introduction

Light is a key environmental factor regulating plant growth and development. Plants possess several classes of photoreceptors, including UV RESISTANCE LOCUS 8 (UVR8) that senses and signals ultraviolet-B radiation (UV-B; Galvao & Fankhauser, 2015; Podolec *et al.*, 2021a). In the model plant *Arabidopsis thaliana* and vegetable crop tomato (*Solanum lycopersicum*), UVR8 regulates a broad range of physiological processes including hypocotyl elongation (Favory *et al.*, 2009; Jenkins, 2017; Yin & Ulm, 2017; Liang *et al.*, 2019; Podolec *et al.*, 2021a). Moreover, the UVR8 pathway is particularly key in promoting plant

survival under UV-B (Kliebenstein *et al.*, 2002; Brown *et al.*, 2005; Favory *et al.*, 2009; Rai *et al.*, 2019; Tissot & Ulm, 2020; Shi & Liu, 2021).

The activities of photoreceptors, including UVR8, are dependent on their subcellular locations within plant cells (Ronald & Davis, 2019). UVR8 is primarily cytosolic, but UV-B induces the nuclear translocation and nuclear accumulation of UVR8 without altering total UVR8 protein levels (Kaiserli & Jenkins, 2007). In the nucleus, UVR8 regulates photomorphogenic responses to UV-B by inducing massive reprogramming of gene transcription (Brown *et al.*, 2005; Favory *et al.*, 2009). UV RESISTANCE LOCUS 8 regulates gene transcription via several different mechanisms, including modulating the abundance or activity of multiple transcriptional regulators (Ulm *et al.*, 2004;

*Joint first authors.

Brown *et al.*, 2005; Brown & Jenkins, 2008; Liang *et al.*, 2018; Y. Yang *et al.*, 2018, 2020; Lau *et al.*, 2019; Sharma *et al.*, 2019; Qian *et al.*, 2020; Tavridou *et al.*, 2020a,b; Podolec *et al.*, 2022; G. Yang *et al.*, 2022). Therefore, unraveling the mechanisms underpinning the UV-B-induced nuclear translocation and accumulation of UVR8 is crucial for understanding early UV-B signaling events.

Ultraviolet-B radiation not only alters the subcellular localization of UVR8, but also induces the photo-switching of UVR8 from a homodimer to a monomer (Rizzini *et al.*, 2011; Christie *et al.*, 2012; D. Wu *et al.*, 2012; Li *et al.*, 2022). UVR8 monomers also can reassociate to form homodimers (Heijde & Ulm, 2013; Heilmann & Jenkins, 2013). In Arabidopsis, two WD40 proteins, REPRESSOR OF UV-B PHOTOMORPHO-GENESIS 1 (RUP1) and RUP2, are critical negative regulators of the UVR8 pathway (Gruber *et al.*, 2010). REPRESSOR OF UV-B PHOTOMORPHOGENESIS proteins interact with UVR8 and accelerate the reassociation of UVR8 monomers into inactive homodimers (Heijde & Ulm, 2013). Under photomorphogenic UV-B, both UVR8 homodimer and monomer are present in plant cells (Heilmann & Jenkins, 2013; Findlay & Jenkins, 2016). However, it is unknown whether UVR8 homodimers or monomers translocate into nucleus.

CONSTITUTIVELY PHOTOMORPHOGENIC 1 (COP1), a repressor of plant photomorphogenesis (Yi & Deng, 2005; Han *et al.*, 2019), is a key player of UVR8-mediated UV-B signaling (Oravecz *et al.*, 2006). CONSTITUTIVELY PHOTOMOR-PHOGENIC 1 interacts with UVR8 in a UV-B-dependent manner (Favory *et al.*, 2009; Rizzini *et al.*, 2011), via two domains in UVR8, the core domain (Crefcoeur *et al.*, 2013; Yin *et al.*, 2015) and a well-conserved C27 domain located within the C-terminus (Cloix *et al.*, 2012; Yin *et al.*, 2015; Lin *et al.*, 2020). Interestingly, RUP1 and RUP2 also interact with UVR8 via the C27 domain (Cloix *et al.*, 2012; Yin *et al.*, 2015), suggesting that COP1 and RUP1/2 may compete for UVR8 binding. We previously reported that COP1 is indispensable for UV-B-induced UVR8 accumulation in the nucleus (Yin *et al.*, 2016). Moreover, RUP1 and RUP2 inhibit the UV-B-induced nuclear accumulation of UVR8 (Qian *et al.*, 2016; Yin *et al.*, 2016). However, the molecular mechanisms of how COP1 and RUP1/2 regulate the nuclear accumulation of UVR8 have remained unknown.

UV RESISTANCE LOCUS 8 does not contain any typical nuclear localization signal (NLS; Kaiserli & Jenkins, 2007; Jenkins, 2017; Yin & Ulm, 2017), whereas COP1 contains a bipartite NLS as well as a nuclear exclusion signal (NES), and is known to show light-dependent nucleocytosolic partitioning (Stacey *et al.*, 1999). UV RESISTANCE LOCUS 8 could enter the nucleus via nuclear import by binding to an NLS-containing protein, such as COP1, or via free diffusion of the UVR8 monomer, a *c.* 47-kDa protein in Arabidopsis (Yin & Ulm, 2017). Based on available observations, particularly the finding that UV-B induces the UVR8–COP1 interaction, three possible models could explain the UV-B-induced nuclear accumulation of UVR8: (1) the UVR8–COP1 heterodimer is imported into the nucleus under UV-B via the NLS of COP1; (2) UVR8 enters the nucleus

independently of COP1, in the nucleus COP1 interacts with UVR8 monomers and promotes their nuclear retention; or (3) COP1 protects UVR8 from degradation in the nucleus.

Here, we provide evidence that, although required for nuclear accumulation, COP1 is not required for the UV-B-induced nuclear translocation of UVR8. Our data indicate that the UV-B-induced photo-switching of UVR8 from a homodimer to a monomer enables the nuclear translocation of UVR8 monomer, probably via free diffusion. In the nucleus, COP1 interacts with UVR8 monomer and promotes its nuclear retention. RUP1 and RUP2 inhibit the nuclear retention of UVR8 by attenuating the UVR8–COP1 interaction, thereby promoting the nuclear exit of UVR8.

Materials and Methods

Plant material, growth conditions and UV-B irradiation

The *Arabidopsis thaliana uvr8-6*, *uvr8-17D* (UVR8^{G101S}), *cop1-4* and *rup1 rup2* mutants are in the Columbia (Col-0) ecotype background (McNellis *et al.*, 1994; Favory *et al.*, 2009; Gruber *et al.*, 2010; Podolec *et al.*, 2021b). The *uvr8-6/35S:YFP-UVR8*, *cop1-4/35S:YFP-UVR8*, *uvr8-6/35S:YFP-UVR8^{W285A}*, *uvr8-6/35:YFP-UVR8^{W285F}*, *uvr8-6/35S:YFP-UVR8*, *uvr8-7/35S:YFP-UVR8^{VP-AA}* Arabidopsis lines were described previously (Heijde *et al.*, 2013; Yin *et al.*, 2015, 2016; YFP, yellow fluorescent protein). The *uvr8-6/35S:YFP-UVR8* line was crossed with *rup1 rup2* to generate *uvr8-6 rup1 rup2/35S:YFP-UVR8*. The synthetic nucleotide fragments of *YFP-YFP-UVR8* and *NLS-YFP-YFP-UVR8* (Fig. S1) were cloned into pDONR207. The sequences were confirmed and cloned into pB7WGY2 (Karimi *et al.*, 2002), yielding *YFP-YFP-YFP-UVR8* and *YFP-NLS-YFP-YFP-UVR8*. The binary vectors were transformed into *uvr8-6* to generate *uvr8-6/35S:YFP-YFP-YFP-UVR8* and *uvr8-6/35S:NLS-YFP-YFP-YFP-UVR8* Arabidopsis lines. A *NLS* or *NES* was added to *COP1* by PCR using primers shown in Table S1. The *NLS-COP1* and *NES-COP1* fragments were cloned into pB7WGY2 (Karimi *et al.*, 2002), yielding *YFP-NLS-COP1* and *YFP-NES-COP1*, respectively. The binary vectors were transformed into *cop1-4* to generate *cop1-4/35S:YFP-NLS-COP1* and *cop1-4/35S:YFP-NES-COP1* Arabidopsis lines. The double mutant *uvr8-17D cop1-4* was generated by genetic crossing. The tomato *sluvr8-1* and *slrup-22* mutants are in the Ailsa Craig wild-type (WT) background (Zhang *et al.*, 2021).

Arabidopsis and tomato seeds were surface-sterilized and sown on half-strength Murashige & Skoog basal salt medium (MS; Duchefa Biochemie, Haarlem, the Netherlands) containing 1% (w/v) sucrose and 1% (w/v) agar (pH = 5.8). The seeds were stratified for 2 d in the dark at 4°C and transferred to a growth chamber with continuous white light (3.6 μmol m^{-2} s^{-1}; −UV-B) or white light supplemented with photomorphogenic UV-B (TL20W/01RS; Philips, Hamburg, Germany; 1.5 μmol m^{-2} s^{-1}) for the indicated periods (Oravecz *et al.*, 2006; Lin *et al.*, 2020). Broadband UV-B treatment was performed with a Philips TL40W/12RS to enhance UVR8 monomerization rapidly as reported previously (Rizzini *et al.*, 2011; Lin *et al.*, 2020).

Protein extraction and immunoblots

Total protein was extracted from the samples with buffer containing 50 mM Tris pH 7.6, 150 mM NaCl, 10% glycerol, 5 mM $MgCl_2$, 0.1% NP-40, 1% DTT, 1% protease inhibitor cocktail (Sigma). The protein extracts were separated by SDS-PAGE and transferred to PVDF membranes according to the manufacturer's instructions (Bio-Rad). To detect UVR8 homodimers, the SDS-PAGE gels were UV-B-irradiated before electrophoretic transfer to PVDF membranes as described previously (Rizzini *et al.*, 2011). Polyclonal anti-UVR8[426-440] (Favory *et al.*, 2009), anti-UVR8[410-424] (Heijde & Ulm, 2013), anti-COP1 (Abiocode, Agoura Hills, CA, USA), anti-GFP (Proteintech, Wuhan, China), anti-histone H3 (Abcam, Shanghai, China), anti-UGPase (Agrisera, Vännäs, Sweden), anti-GADPH (Abmart, Shanghai, China) and anti-Actin (Abmart) antibodies were used as primary antibodies. Horseradish peroxidase (HRP)-conjugated protein A (Pierce, Shanghai, China), anti-rabbit (Abmart) and anti-mouse (Abmart) secondary antibodies were used as required. Signals were detected using a LumiBest ECL reagent solution kit.

Yeast two-hybrid assay

The coding sequences of Arabidopsis *UVR8*, *YFP-UVR8* and *YFP-YFP-YFP-UVR8* were cloned into the pGBKT7 vector as baits. Arabidopsis *COP1* was cloned into the pGADT7 vector as prey. Specific bait and prey constructs were co-transformed into yeast strain AH109. Yeast two-hybrid (Y2H) assays were carried out using the Matchmaker Two-Hybrid System (Clontech; TaKaRa, Tokyo, Japan) according to the manufacturer's protocols. Selection was performed on solid SD/−Leu/−Trp/-His selection medium. Primers used to construct the vectors for Y2H are listed in Table S1.

Cell fractionation

Total proteins were isolated from 7-d-old Arabidopsis or tomato seedlings with lysis buffer (20 mM Tris pH 7.4, 25% glycerol, 150 mM NaCl, 2 mM EDTA, 2.5 mM $MgCl_2$, 250 mM sucrose, 1 mM DTT, 1 mM PMSF). The protein extracts were filtered through three layers of Miracloth. After centrifugation at 1500 *g* for 10 min at 4°C, the supernatants were collected as cytosolic fraction, and the pellet was washed three times with NRBT nucleus resuspension buffer (20 mM Tris pH 7.4, 25% glycerol, 2.5 mM $MgCl_2$, 0.2% Triton X-100). The clean pellet was washed with NRB nucleus resuspension buffer (20 mM Tris pH 7.4, 25% glycerol, 2.5 mM $MgCl_2$). The nuclei were boiled in 5× SDS loading buffer and used for immunoblot analysis. For Fig. 1b, nuclei were incubated with above-mentioned total protein extraction buffer with 0.2% NP-40.

Co-immunoprecipitation (Co-IP)

Total protein extracts were incubated with anti-UVR8[426-440] antibodies. Proteins were extracted with IP buffer (50 mM Tris pH 7.6, 150 mM NaCl, 10% glycerol, 5 mM EDTA, 0.1% NP-40, 1% protease inhibitor cocktail (Sigma)) and incubated at 4°C with slow rotation for 30 min. Following centrifugation at 4°C for 20 min at 14 000 *g*, the clear supernatant was mixed with protein-A beads and incubated at 4°C for 2 h. The agarose beads were washed three times with IP buffer. Proteins were eluted by boiling the beads in 5× SDS loading buffer.

Subcellular localization assay and confocal fluorescence microscopy

The YFP fluorescent signals in epidermal cells of cotyledons or hypocotyls were visualized and imaged using a Leica TCS SP8 microscope (Leica, Shanghai, China) according to the manufacturer's instructions. Yellow fluorescent protein was excited at a wavelength of 514 nm, with an emission wavelength of 525–600 nm.

Fluorescence recovery after photobleaching (FRAP)

Four-days-old seedlings expressing *uvr8-6/35S:YFP-UVR8, cop1-4/35S:YFP-UVR8, cop1-4/35S:YFP-COP1* or *hy5-215/35S:HY5-YFP* were grown in weak white light devoid of UV-B (−UV-B) or supplemented with UV-B under a 304-nm cutoff filter and used for the FRAP assay. Confocal images of YFP in hypocotyls were collected with an LSM 780 confocal laser-scanning microscope (Zeiss) using a water ×40 NA 1.2 C-Apochromat lens. Yellow fluorescent protein was excited at 514 nm, and the emission was collected between 525 and 561 nm with a GaAsP detector (YFP). Pre-bleach and post-bleach images were taken using six slices in a 10-µm *z*-stack range encompassing the nuclei. For photobleaching, 25 iterations and 100% output intensity (514 nm argon laser) were used. For FRAP analyses, single nuclei were defined as regions of interest (ROI). For each experiment, a single pre-bleach 10-µm six-slice *z*-stack was taken, followed by the same z-stack parameters for post-bleach images over the course of 50 cycles at 30 s intervals between cycles. The fluorescence in non-bleached nuclei within the same image plane served as a control. Analyses of YFP intensity were performed with ImageJ.

Fluorescence loss in photobleaching

Fluorescence loss in photobleaching (FLIP) assays were performed using 4-d-old seedlings expressing *uvr8-6/35S:YFP-UVR8* or *uvr8-6 rup1rup2/35S:YFP-UVR8* grown in weak white light and treated with 20 min of broadband UV-B under a 304-nm cutoff filter. Confocal images of YFP in cotyledons were collected with an FV3000 confocal laser-scanning microscope (Olympus, Shanghai, China) using a ×20 objective lens. YFP was excited at 488 nm and the emission was collected between 525 and 600 nm. For photobleaching of cytosol, a 50% output intensity (488 nm argon laser) for 500 ms was used. For FLIP analysis, single nuclei of bleached cells were defined as ROI. For each experiment, two pre-bleach images were taken, followed by one bleaching image and 77 post-bleach images over the course of 80 cycles at 2.17-s intervals between cycles. The fluorescence in nuclei of nonbleached cells within the same image plane served as a control.
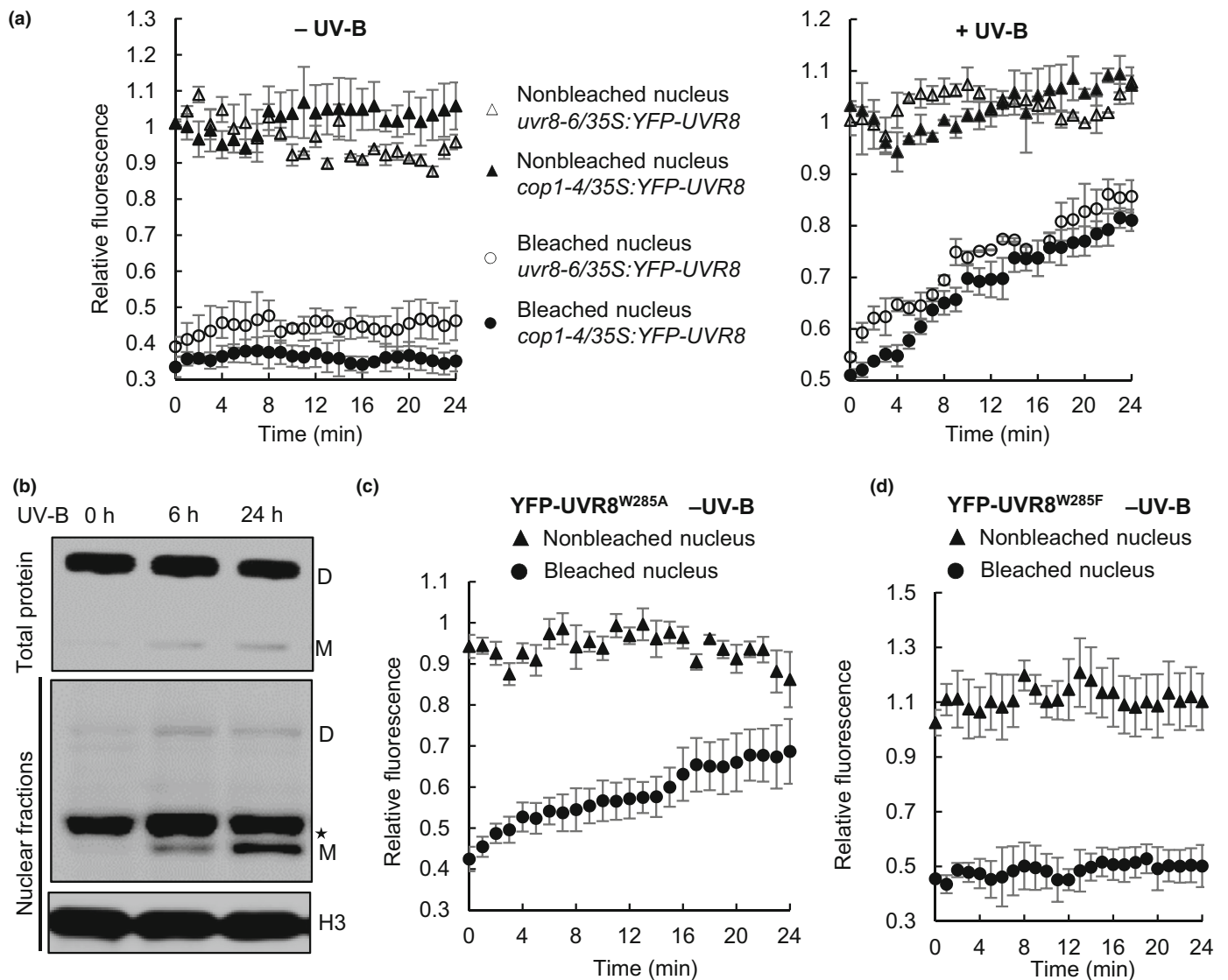
Fig. 1 Ultraviolet-B radiation (UV-B) induces the nuclear translocation and nuclear accumulation of UV RESISTANCE LOCUS 8 (UVR8) monomer. (a) Ultraviolet-B radiation induces the nuclear translocation of UVR8 fused to yellow fluorescent protein (YFP-UVR8). Fluorescence recovery after photobleaching (FRAP) assays were performed with 4-d-old Arabidopsis seedlings of the indicated genotype grown in white light (–UV-B) or white light supplemented with UV-B for 24 h (+UV-B). After bleaching the nucleus, the recovery of fluorescence in the bleached nucleus was recorded (circles). Nonbleached nuclei (triangles) served as controls. The experiments were repeated three times with similar results and three nuclei in one experiment are shown. Error bars represent ± SEM ($n = 3$). (b) Ultraviolet-B radiation induces UVR8 monomer accumulation in the nucleus. Four-days-old wild-type Arabidopsis seedlings were grown in white light (0 h UVB) or white light supplemented with UV-B for 6 and 24 h as indicated. Immunoblot analysis was performed with nonheat-denatured total protein extracts and nuclear fractions to detect UVR8 homodimer (D) and monomer (M) with anti-UVR8[410-424]. The asterisk indicates a nonspecific band. Histone H3 served as a nuclear loading control. The negative control *uvr8-6* is included in Fig. S3. (c, d) YFP-UVR8[W285A] but not YFP-UVR8[W285F] translocate into the nucleus under white light treatment. FRAP assays with *uvr8-6/35S:YFP-UVR8[W285A]* (c) and *uvr8-6/35S:YFP-UVR8[W285F]* (d) Arabidopsis seedlings grown in white light. After bleaching the nucleus, the recovery of fluorescence in the bleached nucleus was recorded (circles). Nonbleached nuclei (triangles) served as controls. The experiments were repeated three times with similar results and three nuclei in one experiment are shown. Error bars represent ± SEM ($n = 3$).

RNA extraction and quantitative reverse transcription-PCR analysis

Total RNA was isolated from Arabidopsis seedings with a Plant RNA Extraction kit (OMEGA, Norcross, GA, USA) according to the manufacturer's instructions. Reverse transcription was carried out with cDNA synthesis SuperMix with gDNA remover (TransGen, Beijing, China). qPCR was performed with Fast SYBR Green Master Mix (TransGen) on a CFX96 Real-time PCR machine (Bio-Rad). The *18S* rRNA gene was used as an internal control. Primers used are listed in Table S1.

Statistical analysis

Statistics used in this article are indicated in respective figure legends.

New
Phytologist

Accession numbers

Sequence data from this article can be retrieved from the Arabidopsis Genome Initiative or GenBank/EMBL databases under the following accession numbers: At5g63860 (*UVR8*), At2g32950 (*COP1*), At5g11260 (*HY5*), At5g52250 (*RUP1*) and At5g23730 (*RUP2*).

Results

COP1 is not required for UV-B-induced rapid nuclear translocation of UVR8

In order to test whether the nuclear translocation of UVR8 requires COP1, we performed FRAP assays using previously established Arabidopsis transgenic lines expressing a YFP-UVR8 fusion protein in the presence or absence of functional COP1 (Yin *et al.*, 2016). For this we took advantage of the COP1-4 allele that has a premature stop codon at the position of Gln-283; thus *cop1-4* expresses a truncated protein containing only the N-terminal 282 amino acids including the NLS but lacking the WD40 repeats responsible for interaction with UVR8 (McNellis *et al.*, 1994; Favory *et al.*, 2009; Wang *et al.*, 2022). It should be noted that although *cop1-4* is a nonlethal, weak *cop1* allele (McNellis *et al.*, 1994; Ordonez-Herrera *et al.*, 2015), UV-B signaling is essentially abolished in *cop1-4* (Oravecz *et al.*, 2006; Favory *et al.*, 2009).

Although low amounts of UVR8 can be detected in the nucleus in the absence of UV-B (Kaiserli & Jenkins, 2007; Qian *et al.*, 2016; Yin *et al.*, 2016), no significant nuclear translocation of YFP-UVR8 was observed in white light in our FRAP assays over the timescale of the experiment (Fig. 1a). Surprisingly, however, UV-B induced the nuclear translocation of YFP-UVR8 in both WT and *cop1-4* mutant backgrounds (Fig. 1a). As a negative control, we performed FRAP with Arabidopsis expressing a HY5-YFP fusion protein. Consistent with the fact that HY5 is a constitutively nuclear protein, there was no recovery of fluorescence after photobleaching of the nucleus; that is, no nuclear translocation of HY5-YFP was observed in the absence or presence of UV-B over the time scale of the experiment (Fig. S2). Thus, we conclude that, although required for UVR8 nuclear accumulation in response to UV-B (Yin *et al.*, 2016), COP1 is not required for the UV-B-induced rapid nuclear translocation of UVR8.

UV-B-induced nuclear translocation of UVR8 monomers probably can occur via free diffusion

Because UVR8 exists as a homodimer in Arabidopsis in white light, and UV-B induces the dissociation of homodimers into monomers, we reasoned that UVR8 might translocate into the nucleus as a monomer. To test this possibility, we subjected Arabidopsis seedlings to photomorphogenic UV-B treatment, which monomerizes only a small fraction of the total UVR8 pool, and examined which form of UVR8 accumulates in the nucleus (Figs 1b, S3). Although the majority of total cellular UVR8

existed as a homodimer under UV-B irradiation, UVR8 monomer was dominant in the nucleus, supporting the hypothesis that UVR8 monomers translocate into the nucleus (Fig. 1b). UVR8^{W285A} and UVR8^{W285F} are both nonresponsive to UV-B due to mutation of the W285 key residue (Rizzini *et al.*, 2011; O'Hara & Jenkins, 2012; Heijde *et al.*, 2013; Huang *et al.*, 2014). However, UVR8^{W285A} shows weak constitutive activity, probably associated with its only weak homodimeric conformation and thus possibly being partially monomeric *in vivo*, UVR8^{W285F} exists as constitutive homodimer (Rizzini *et al.*, 2011; O'Hara & Jenkins, 2012; Heijde *et al.*, 2013; Huang *et al.*, 2014). Nuclear translocation of YFP-UVR8^{W285A} but not YFP-UVR8^{W285F} was observed in FRAP assays of plants grown in white light (Fig. 1c,d), consistent with the notion that UVR8 translocates into the nucleus in a monomer form.

UV RESISTANCE LOCUS 8 monomers might enter the nucleus via facilitated nuclear import or via free diffusion. The calculated molecular mass of Arabidopsis UVR8 monomer is *c.* 47 kDa. Independent research provided evidence that soluble proteins with molecular weight beyond 60 kDa can enter the nucleus via free diffusion in the physiologically relevant time scale (Wang & Brattain, 2007; Popken *et al.*, 2015; Timney *et al.*, 2016). We reasoned that if UVR8 monomers enter the nucleus via free diffusion, adding a large protein tag without NLS would prevent the UV-B-induced nuclear accumulation of UVR8. Therefore, we generated transgenic Arabidopsis lines expressing the YFP-YFP-YFP-UVR8 fusion protein in the *uvr8* mutant background. The molecular mass of YFP-YFP-YFP-UVR8 monomer is >130 kDa, which is most likely beyond the molecular mass limit for free diffusion into nucleus within physiologically relevant timescale. We analyzed whether YFP-YFP-YFP-UVR8 could form homodimers and respond to UV-B. The YFP-YFP-YFP-UVR8 fusion protein was detected as a high molecular mass band and a lower molecular mass band in nonheat-denatured protein extracts from Arabidopsis grown in white light and UV-B light, respectively (Fig. S4a). As established previously for UVR8 (Rizzini *et al.*, 2011), the larger of these two bands can be considered to be YFP-YFP-YFP-UVR8 homodimer and the lower band YFP-YFP-YFP-UVR8 monomer (Fig. S4a). In agreement with this notion, only a single band corresponding to YFP-YFP-YFP-UVR8 monomer was detected from heat-denatured protein.

Extracts (Fig. S4a). Moreover, YFP-YFP-YFP-UVR8 retained the ability to interact with COP1 in a UV-B-dependent manner in Y2H assays (Fig. S4b). Thus, the triple YFP tag fusion protein retained the protein folding and other properties of UVR8.

We then analyzed whether UV-B would induce the nuclear accumulation of the YFP-YFP-YFP-UVR8 fusion protein in plants. YFP-UVR8 localized to both the cytosol and nucleus in white light, and UV-B induced its accumulation in the nucleus, yet the YFP-YFP-YFP-UVR8 fusion protein localized to the cytosol and no nuclear signal could be detected, even in the presence of UV-B (Fig. 2a). As a positive control we generated lines expressing an YFP-NLS-YFP-YFP-UVR8 fusion protein, which localized to the nucleus under both white light and UV-B treatment (Fig. 2a). Immunoblotting analysis confirmed that UV-B
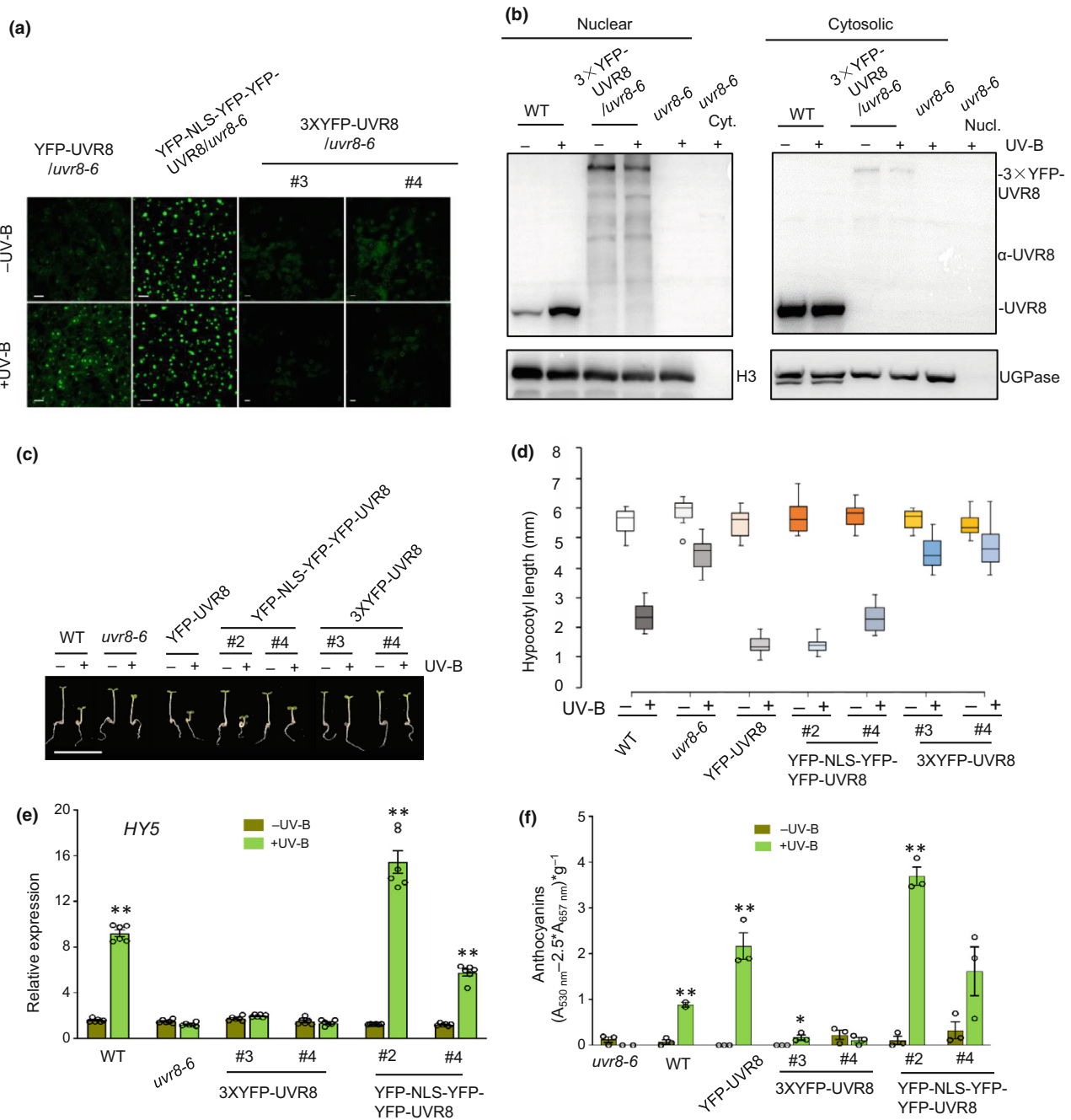
Fig. 2 Fusion of triple yellow fluorescent protein (YFP) tag to UV RESISTANCE LOCUS 8 (UVR8) strongly impairs its ultraviolet-B radiation (UV)-B-induced nuclear accumulation. (a, b) Fusion with triple YFP disrupts the UV-B-induced nuclear accumulation of UVR8. (a) Subcellular localization of the YFP-YFP-YFP-UVR8 fusion protein. YFP fluorescence in the cotyledon adaxial epidermis of 4-d-old *uvr8-6/35S:YFP-UVR8, uvr8-6/35S:YFP-YFP-YFP-UVR8* and *uvr8-6/35S:YFP-NLS-YFP-YFP-UVR8* seedlings. Seedlings were grown in white light (–UV-B) or white light supplemented with UV-B (+UV-B) for 24 h. Bar, 10 μm. (b) Immunoblot analysis of cytosolic and nuclear proteins of 7-d-old Arabidopsis seedlings grown in white light (–UV-B) or white light supplemented with UV-B for 24 h (+UV-B) probed with anti-UVR8$^{426-440}$, anti-histone H3 (nuclear control) and anti-UGPase antibodies (cytosolic control). WT, wild type. (c, d) Representative image (c) and quantification (d) of hypocotyl length in the WT, *uvr8-6, uvr8-6/35S:YFP-UVR8, uvr8-6/35S:YFP-YFP-YFP-UVR8* and *uvr8-6/35S:YFP-NLS-YFP-YFP-UVR8* seedlings grown in white light (−) or white light supplemented with UV-B (+) for 4 d. In (d) the median (the horizontal line), the lower quartile, the upper quartile and the minimum point and maximum point are included in each box ($n = 15$). One outlier is represented by an open circle. $P < 0.05$ for 3XYFP-UVR8 #4, $P < 0.01$ for all the rest from Student's t-test (-UVB vs +UVB for each genotype). Bar, 1 cm in Fig. 2c. (e) UV-B fails to induce *HY5* transcription in *uvr8-6/35S:3XYFP-UVR8* Arabidopsis lines. Quantitative reverse transcription (qRT) PCR analysis of *HY5* transcripts in 4-d-old seedlings grown in white light (–UV-B) or white light supplemented with UV-B for 2 h (+UV-B). The value for the WT treated with white light was set to 1. Means and ± SE of six biological samples are shown. Each open circle represents one datum. (f) Ultraviolet-B radiation fails to induce anthocyanin accumulation in *uvr8-6/35S:YFP-YFP-YFP-UVR8* Arabidopsis lines. Anthocyanin levels were quantified in seedlings grown in white light (–UV-B) or white light supplemented with UV-B (+UV-B). Mean and ± SE of three biological samples are shown. Each open circle represents one data point. **, $P < 0.01$; *, $P < 0.05$ (Student's t-test to compare-UVB and + UVB for each genotype). No asterisks indicate not significant.

did not induce the nuclear accumulation of the YFP-YFP-YFP-UVR8 fusion protein, albeit low levels were detected in the nuclear fraction (Fig. 2b). Thus, adding triple YFP tag to UVR8 strongly impaired the UV-B-induced nuclear accumulation of UVR8. These observations suggest that the UV-B-induced nuclear translocation of UVR8 occurs via free diffusion.

We tested whether YFP-YFP-YFP-UVR8 Arabidopsis lines would exhibit typical UV-B-induced photomorphogenesis. Hypocotyl elongation was efficiently inhibited by UV-B in the WT and a *uvr8-6/35S:YFP-UVR8* complementation line, but not in the *uvr8-6/35S:YFP-YFP-YFP-UVR8* lines (Fig. 2c,d). By contrast, however, the *uvr8-6/35S:YFP-NLS-YFP-YFP-UVR8* lines exhibited strong inhibition of hypocotyl elongation under UV-B, suggesting that the triple YFP tag did not abolish the activity of UVR8 (Fig. 2c,d). Likewise, the expression of the UV-B marker gene *HY5* and anthocyanin accumulation were induced by UV-B in the YFP-NLS-YFP-YFP-UVR8 control lines, but not in the YFP-YFP-YFP-UVR8 expressing lines (Fig. 2e,f). Thus, adding triple YFP tag strongly impaired the nuclear accumulation of UVR8 and thereby UV-B signaling, both of which could be restored by adding an NLS.

Nucleus-localized COP1 promotes UV-B-induced nuclear accumulation of UVR8

Based on the notion that COP1 is not required for the UV-B-induced nuclear translocation of UVR8, together with the observation that UVR8 protein levels are not altered by UV-B or COP1 (Fig. S5a; Oravecz *et al.*, 2006; Kaiserli & Jenkins, 2007; Yin *et al.*, 2016), we postulated that nucleus-localized COP1 regulates the nuclear accumulation of UVR8. To test this possibility, we took advantage of a strong viral NLS and NES, as reported previously (Kaiserli & Jenkins, 2007). We generated Arabidopsis lines expressing YFP-NLS-COP1 or YFP-NES-COP1 in the *cop1-4* background, as no UV-B-induced nuclear accumulation of UVR8 can be detected in this mutant (Yin *et al.*, 2016).

For unknown reasons, YFP-NES-COP1 fusion protein levels were much higher than YFP-NLS-COP1 fusion protein levels in multiple independent plant lines (Fig. S5b). UVR8 protein levels in the YFP-NLS-COP1 and YFP-NES-COP lines are similar under both white light and UV-B (Fig. S5a). The YFP-NLS-COP1 fusion protein localized to the nucleus, forming typical photobodies in white light, and UV-B enhanced its nuclear accumulation (Fig. 3a). By contrast, YFP-NES-COP1 fusion protein constitutively localized to the cytosol, forming cytosolic inclusion bodies similar as reported previously (Stacey *et al.*, 1999).

Interestingly, UV-B did not alter YFP-NES-COP1 protein levels (Fig. 3a). Therefore, these *YFP-NLS-COP1* and *YFP-NES-COP1* Arabidopsis lines could be used to distinguish whether COP1 acts in the nucleus or cytosol to regulate the UV-B-induced nuclear accumulation of UVR8. Ultraviolet-B radiation induced the nuclear accumulation of UVR8 in the *YFP-NLS-COP1* lines, which was accompanied by a slight decrease in UVR8 levels in the cytosol (Fig. 3b). By contrast, UV-B failed to induce the nuclear accumulation of UVR8 in the *YFP-NES-*

COP1 lines (Fig. 3b). We conclude that nucleus-localized COP1 promotes UV-B-induced nuclear retention and thus accumulation of UVR8.

In white light, *YFP-NLS-COP1*, but not *YFP-NES-COP1*, complemented the dwarf phenotype of *cop1-4* (Fig. 3c), which is consistent with the notion that COP1 inhibits photomorphogenesis in the nucleus (von Arnim & Deng, 1994; Qin *et al.*, 2020). Ultraviolet-B radiation efficiently inhibited hypocotyl elongation in seedlings of the *YFP-NLS-COP1* lines, but not the *YFP-NES-COP1* lines (Fig. 3c). Moreover, UV-B promoted *HY5* expression in the *YFP-NLS-COP1* lines, but not in the *YFP-NES-COP1* lines (Fig. 3d). Collectively, these results indicate that nucleus-localized COP1 promotes the nuclear accumulation of UVR8 and UV-B signaling.

We then asked how nucleus-localized COP1 promotes the nuclear accumulation of UVR8. UVR8 protein levels appear to be affected neither by UV-B (Kaiserli & Jenkins, 2007; Heijde & Ulm, 2013; Heilmann & Jenkins, 2013), nor by COP1 (Fig. S5a; Oravecz *et al.*, 2006; Yin *et al.*, 2016). We hypothesized that nucleus-localized COP1 binds to UVR8 to promote the nuclear retention of this photoreceptor. Indeed, YFP-NLS-COP1 formed protein complexes with UVR8 in plants in response to UV-B as revealed by Co-IP assays (Fig. 3e). Notably, YFP-NES-COP1 also formed protein complexes with UVR8 in plants under UV-B (Fig. 3e), which is consistent with our previous finding that UVR8 interacts with COP1 both in nucleus and cytosol (Yin *et al.*, 2016). Moreover, the substitutions of valine (410) and proline (411) residues located at UVR8 C-terminus with alanine, UVR8[VP-AA], leads to decreased UV-B-induced UVR8–COP1 interaction (Yin *et al.*, 2015), and UVR8 nuclear accumulation (Fig. 4), confirming that UVR8–COP1 interaction is critical for UVR8 nuclear accumulation. We conclude that although UVR8 interacts with COP1 both in the cytosol and nucleus, nuclear COP1 is required for nuclear retention of UVR8, as well as UVR8 signaling.

RUP1 and RUP2 inhibit the nuclear retention of UVR8 by inhibiting the UVR8–COP1 interaction

In order to understand UVR8 nucleocytosolic partitioning dynamics, we treated Arabidopsis seedlings with UV-B for 24 h to induce the nuclear accumulation of UVR8 and transferred them to white light for recovery. In the WT, nuclear UVR8 levels were enhanced by UV-B treatment and strongly decreased at 3 h post UV-B treatment, eventually reaching a level comparable to the starting point at 7 h post-UV-B treatment (Fig. 5a). UV RESISTANCE LOCUS 8 levels in the cytosol were complementary to those in the nucleus, showing opposite patterns (Fig. 5a). Thus, UVR8 exits the nucleus following the cessation of UV-B treatment. Co-immunoprecipitation assays revealed that the UVR8–COP1 interaction was induced by UV-B and was rapidly attenuated during recovery in white light in the WT (Fig. 5b; Heijde & Ulm, 2013); this pattern is positively correlated with the nuclear retention of UVR8.

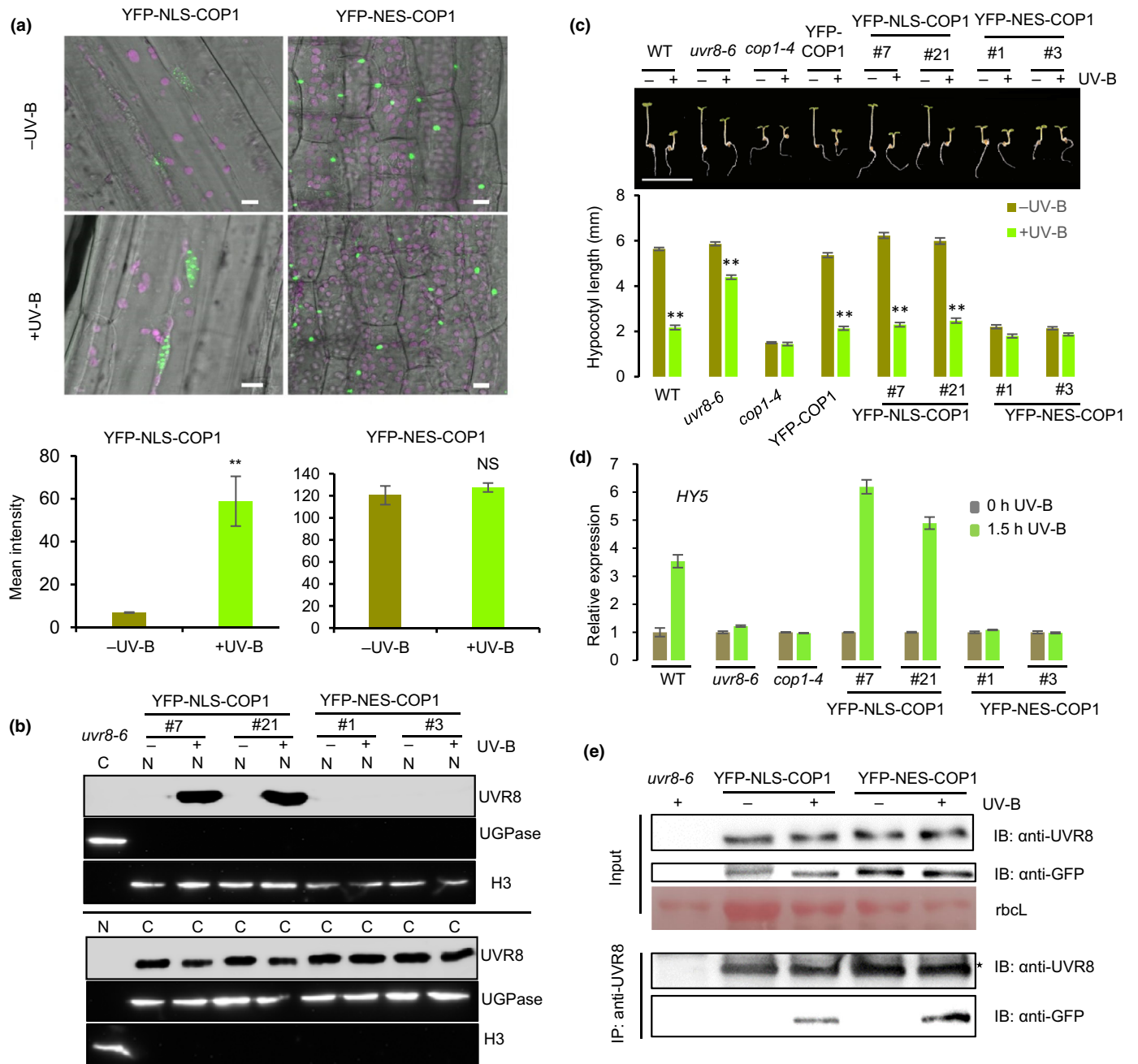REPRESSOR OF UV-B PHOTOMORPHOGENESIS 1 and RUP2 interact with the C27 domain of UVR8, which also

Fig. 3 Nuclear CONSTITUTIVELY PHOTOMORPHOGENIC 1 (COP1) promotes UV-B-induced nuclear accumulation of UV RESISTANCE LOCUS 8 (UVR8) and UV-B signaling. (a) Top: Subcellular localization of COP1 protein in *cop1-4/35S:YFP-NLS-COP1* and *cop1-4/35S:YFP-NES-COP1* Arabidopsis in white light (−UV-B) or white light supplemented with UV-B (+UV-B). Bar, 20 µm. Bottom: Mean fluorescence intensity of YFP-NLS-COP1 and YFP-NES-COP1. Mean and ± SE from $n \geqq 6$ images with the same magnification factor from different hypocotyls. Green and magenta color represent YFP fluorescence and chloroplast autofluorescence, respectively. Bar, 10 µm. **, $P < 0.01$ (two-tailed Student's t-test), ns, not significant. (b) Nuclear COP1 promotes UV-B-induced nuclear accumulation of UVR8. Seven-days-old *cop1-4/35S:YFP-NLS-COP1* and *cop1-4/35S:YFP-NES-COP1* Arabidopsis grown in white light (−) or white light supplemented with UV-B (+) for 12 h. Immunoblotting analysis was performed with anti-UVR8[426-440], anti-histone H3 (nuclear control) and anti-UGPase antibodies (cytosolic control). (c, d) Nuclear COP1 promotes UV-B responses. (c) Four-days-old WT, *uvr8-6*, *cop1-4*, *cop1-4/35S: YFP-COP1*, *cop1-4/35S:YFP-NLS-COP1* and *cop1-4/35S:YFP-NES-COP1* seedlings grown in white light (−) or white light supplemented with UV-B (+). Images of representative individuals (upper panel) and hypocotyl lengths (lower panel) are shown. Mean and ± SE are shown ($n = 15$). Bar, 1 cm. **, $P < 0.01$ (Student's t-test). (d) Quantitative reverse transcription (qRT)-PCR analysis of *HY5* transcript levels in 4-d-old wild-type (WT), *uvr8-6*, *cop1-4*, *cop1-4/35S:YFP-NLS-COP1* and *cop1-4/35S:YFP-NES-COP1* seedlings grown in white light (0 h) or white light supplemented with UV-B for 1.5 h. The value for WT treated with white light was set to 1. Mean and SE of three biological samples are shown. (e) Coimmunoprecipitation analysis for the detection of UVR8–COP1 interaction with 7-d-old *cop1-4/YFP-NLS-COP1* and *cop1-4/YFP-NES-COP1* seedlings that grew either under white light (−) or white light supplemented with UV-B (+) for 12 h. Anti-UVR8[426-440] antibody was used for immunoprecipitation. Immunoblotting analyses were performed with anti-UVR8[426-440] and anti-GFP antibodies. The asterisk indicates a nonspecific band.
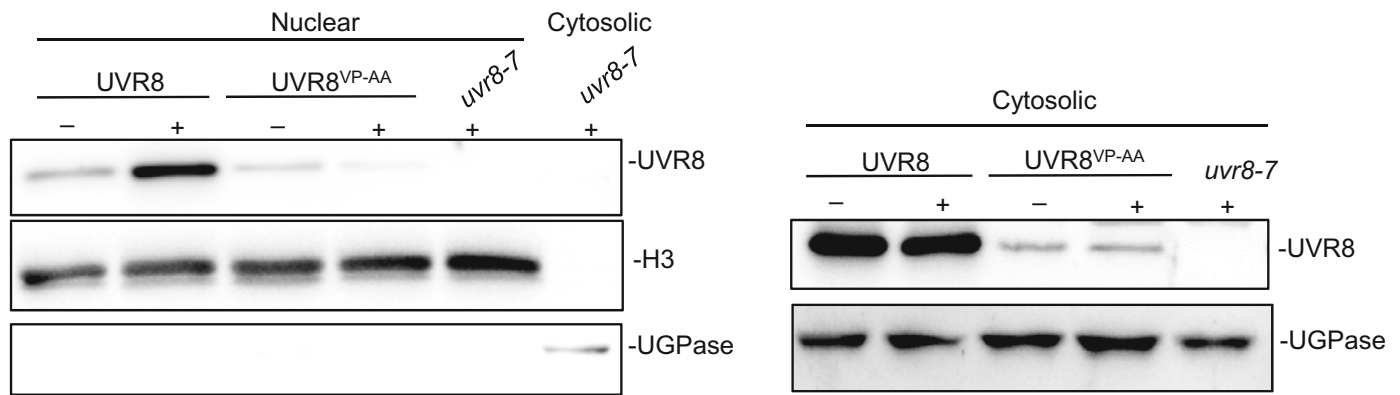
Fig. 4 The Ultraviolet-B radiation (UV-B)-induced UV RESISTANCE LOCUS 8 (UVR8) nuclear accumulation is strongly reduced in $UVR8^{VP-AA}$ Arabidopsis mutant. Immunoblot analysis with Anti-UVR8$^{426-440}$, anti-UGPase (cytosolic marker) and anti-Histone H3 (nuclear marker) in nuclear and cytosolic fractions from 7-d-old uvr8-7/35S:UVR8 (UVR8), uvr8-7/35S:UVR8^{VP-AA} (line #11) and uvr8-7 seedlings grown in white light (−) or white light supplemented with UV-B for 24 h (+).

mediates the interaction of UVR8 with COP1 (Gruber et al., 2010; Cloix et al., 2012; Yin et al., 2015). The UVR8–COP1 interaction was maintained at high levels for much longer periods in the rup1 rup2 double mutant than in the WT following the cessation of UV-B treatment (Fig. 5b), which is consistent with previous observations (Heijde & Ulm, 2013). These results indicate that RUP1 and RUP2 interfere with the UVR8–COP1 interaction. Nuclear UVR8 also was maintained at high levels for a much longer period following the cessation of UV-B irradiation in the rup1 rup2 double mutant than in the WT (Fig. 5b). Conversely, cytosolic UVR8 was maintained at low levels after UV-B treatment in rup1 rup2 (Fig. 5c). To analyze the nuclear exit of UVR8 post UV-B treatment, we performed FLIP assays. The decline of the nuclear YFP-UVR8 occurred much more slowly in rup1 rup2 than in the WT (Fig. 5d).

We reason that RUP1 and RUP2 may inhibit UVR8 nuclear retention via inhibiting UVR8–COP1 interaction or promoting the nuclear exit of UVR8 independent of COP1. To further investigate the function of RUP1 and RUP2, we generated the cop1-4 rup1 rup2 triple mutant by genetic crossing. We found that UV-B could not induce UVR8 nuclear accumulation in cop1-4 rup1 rup2 triple mutant plants (Fig. 5e), suggesting that the effect of RUP1 and RUP2 on UVR8 nuclear accumulation is dependent on COP1.Collectively, we conclude that RUP1 and RUP2 inhibit the nuclear retention of UVR8 by inhibiting the UVR8–COP1 interaction.

Tomato UVR8 (SlUVR8) regulates UV-B photomorphogenesis and UV-B stress tolerances (Liu et al., 2020). We recently reported that tomato RUP (SlRUP) is a functional ortholog of Arabidopsis RUP1 and RUP2 (Zhang et al., 2021). UV-B induced the nuclear accumulation of Tomato UVR8 (SlUVR8) in the WT and nuclear SlUVR8 levels declined post UV-B irradiation (Fig. S6). We noticed that UV-B-induced nuclear accumulation of Arabidopsis UVR8 is much more pronounced than SlUVR8 in the respective WT plants. Nuclear SlUVR8 levels were much higher in slrup than in the WT under UV-B and post UV-B treatment at each time point (Fig. S6). Thus, SlRUP inhibits the nuclear retention or SlUVR8 in tomato (Fig. S6). These results indicate that the role of RUP proteins in the regulation of the nuclear retention of UVR8 is well conserved in Arabidopsis and tomato.

Discussion

Light regulates the subcellular localizations of several plant photoreceptors to adjust their activities during photomorphogenesis (Sakamoto & Briggs, 2002; Chen et al., 2005; Hiltbrunner et al., 2005; Kong et al., 2006; Kaiserli & Jenkins, 2007; Genoud et al., 2008; Rausenberger et al., 2011; Pfeiffer et al., 2012; Klose et al., 2015). Available evidence points to the nucleus as the primary site of UVR8 action (Kaiserli & Jenkins, 2007; Qian et al., 2016; Yin et al., 2016). In the current study, we demonstrated that UVR8 shuttles between the cytosol and nucleus based on the availability of UV-B. This is analogous to the red/far-red light induced shuttling of phytochrome A between the cytosol and nucleus (Rausenberger et al., 2011). However, the mechanism underlying the nucleocytosolic distribution of UVR8 remained unclear. Here we show that a UV-B-induced conformational change in UVR8 from a homodimer to monomer facilitates the nuclear translocation of UVR8 (Fig. 5f). UVR8 monomer can translocate into the nucleus independent of COP1 binding. In the nucleus, COP1 interacts with UVR8 to promote UVR8 nuclear retention. RUP1 and RUP2 inhibit UVR8 nuclear retention via inhibiting UVR8–COP1 interaction.

Previously, we reported that UV-B-induced UVR8 accumulation in the nucleus requires COP1 with unknown mechanisms (Yin et al., 2016). Current work is consistent with our previous report showing that COP1 is required for UV-B-induced nuclear accumulation of UVR8, and further revealed the mechanisms of COP1 in this process. Under the artificial mammalian glucocorticoid receptor (GR)-COP1 fusion system, UVR8 interacts with GR-COP1 under UV-B in the cytosol and can be co-imported into nucleus in the presence of dexamethasone, a chemical ligand for GR (Yin et al., 2016). This co-import model is further supported by the fact that COP1 contains an NLS, whereas no NLS could be identified in UVR8. However, the artificial GR-COP1
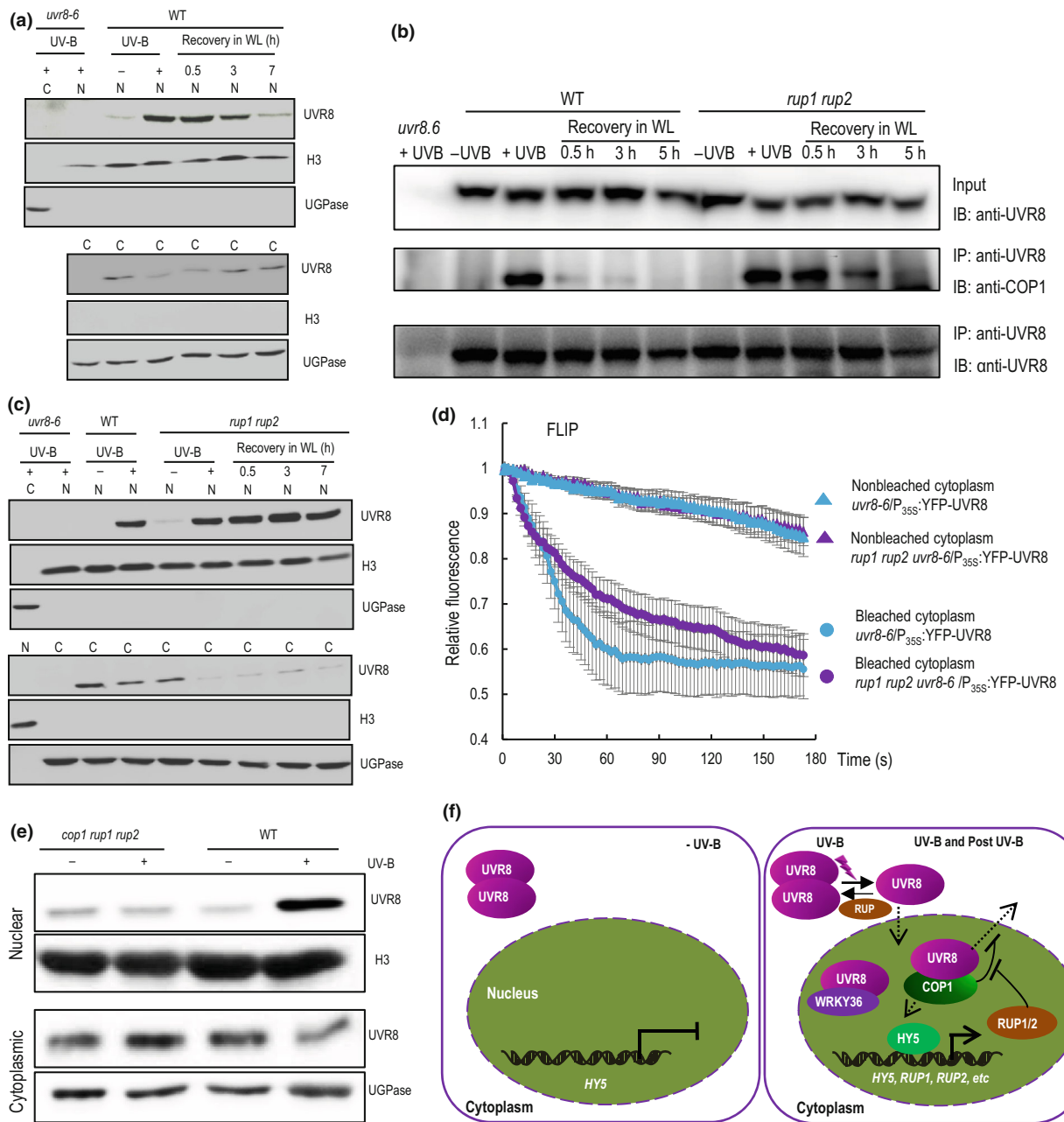
Fig. 5 REPRESSOR OF UV-B PHOTOMORPHOGENESIS 1 (RUP1) and RUP2 inhibit UV RESISTANCE LOCUS 8 (UVR8) nuclear retention. (a) UVR8 is a nucleocytosolic shuttling protein. Wild-type (WT) plants grown in white light (−) or white light supplemented with UV-B for 24 h (+), followed by recovery in white light for different periods as indicated. N and C represent the nuclear and cytosolic protein fraction, respectively. Immunoblotting analysis was performed with anti-UVR8[426-440], anti-histone H3 (nuclear control) and anti-UGPase antibodies (cytosolic control). (b) Coimmunoprecipitation of CONSTITUTIVELY PHOTOMORPHOGENIC 1 (COP1) with UVR8 antibody from total protein extracts of WT and *rup1rup2*. Seven-days-old seedlings were treated with UV-B for 24 h and broadband UV-B for 30 min, followed by recovery in white light (WL) for the indicated periods. Anti-UVR8[426-440] antibody was used for immunoprecipitation. Immunoblotting analyses were performed with anti-UVR8[426-440] and anti-COP1 antibodies. (c) Following UV-B treatment, nuclear UVR8 levels decline, which is delayed in the *rup1 rup2* mutant. Plant growth conditions and immunoblotting are exactly as shown in (a). (d) RUP1 and RUP2 promote the nuclear exit of UVR8 following UV-B treatment. Fluorescence loss in photobleaching (FLIP) assays were performed with Arabidopsis seedlings grown in white light supplemented with UV-B for 20 min. After bleaching the cytosol, the loss of the fluorescence in the nucleus was recorded (circles). The nuclei of nonbleached cells (triangles) served as controls. $n > 10$. Error bars represent ± SEM. (e) The role of RUP1 and RUP2 in UVR8 nuclear accumulation is dependent on COP1. WT and *cop1 rup1 rup2* plants grown in white light (−) or white light supplemented with UV-B for 24 h. Immunoblotting analysis was performed with anti-UVR8[426-440], anti-histone H3 (nuclear control) and anti-UGPase antibodies (cytosolic control). (f) Proposed model of the UV-B induced UVR8 monomerization and its nuclear translocation, and the roles of COP1, RUP1 and RUP2 in the regulation of UVR8 nuclear retention. In cytosol, UV-B induces UVR8 monomerization. UVR8 monomer translocate into nucleus most probably via free diffusion. In the nucleus, COP1 binds to UVR8 monomer and promotes UVR8 nuclear retention. RUP1 and RUP2 promote UVR8 nuclear exit via inhibiting UVR8–COP1 interaction. In addition, UVR8 also interacts with several transcription factors including WRKY36 in the nucleus. The solid and dashed arrows indicate stimulation and the blunt-ended arrows indicate inhibition.

system primarily shows that a co-import mechanism is possible, but not that this is the main mechanism in a WT setting. Here we show that UV-B-induced UVR8 rapid nuclear translocation can occur independently of binding to COP1(Fig. 1). Consistently, UV-B-induced nuclear accumulation of COP1 (taking c. 24 h) was shown to be much slower than that of UVR8 (taking only minutes to a few hours; Oravecz et al., 2006; Kaiserli & Jenkins, 2007). Yet, our FRAP data do not exclude the possibility that UVR8 translocate into nucleus with co-import model through interaction with other protein containing an NLS, such as one of the UVR8-interacting transcription factors (Liang et al., 2018; Yang et al., 2018, 2020; Qian et al., 2020). The proposed free diffusion model and a co-import model via an unknown protein for UV-B induced UVR8 nuclear translocation are not mutually exclusive and can happen in parallel. It is of note that the possible COP1-independent co-imported UVR8 would eventually require COP1 for its nuclear retention and nuclear accumulation. However, addition of triple YFP tag prevented UV-B-induced UVR8 nuclear accumulation, which does not support a co-import model.

Both UV-B-treated YFP-UVR8 fusion protein and the constitutively partially monomeric YFP-UVR8^{W285A} translocated into the nucleus, whereas the constitutive dimer YFP-UVR8^{W285F} and non-UV-B-treated YFP-UVR8 did not, suggesting that UVR8 translocates into the nucleus in a monomer form. Indeed, previous work reported that YFP-UVR8^{W285F} and UVR8^{W285F} are deficient in nuclear accumulation (Qian et al., 2016; Yin et al., 2016). Supporting this finding, total cellular UVR8 protein is primarily homodimeric but nuclear UVR8 protein is predominantly monomeric in Arabidopsis seedlings treated with a low fluence rate of UV-B (Fig. 1b; Qian et al., 2016). It is of note that residual levels of UVR8 homodimer were detected in nucleus from non-UV-B-treated plant materials (Fig. 1b; Kaiserli & Jenkins, 2007; Qian et al., 2016; Yin et al., 2016). It is possible that a small fraction of (newly synthesized) UVR8 monomers translocate into nucleus before they could form homodimer in cytosol. These escaped UVR8 monomers form homodimers in the nucleus. We propose that UV-B induces the dissociation of UVR8 homodimers into monomers, which facilitates their nuclear translocation (Fig. 5f). The role of conformational changes in facilitating the nuclear translocation of proteins also was identified for the SA receptor NONEXPRESSOR OF PR GENES 1 (NPR1; Kinkema et al., 2000; Y. Wu et al., 2012). Inactive NPR1 oligomers reside in the cytosol. SA induces the switch of NPR1 from an oligomer to a monomer, which facilitates its nuclear translocation (Tada et al., 2008).

Protein traverses the nuclear pore complexes (NPCs) through either passive diffusion or facilitated transport systems (Grossman et al., 2012; Timney et al., 2016). Small protein can transverse the NPCs via free diffusion, and large protein via facilitated nuclear import. The prevailing view for the functional model of passive transport through NPCs is that have a barrier size threshold of 60 kDa for passive diffusion (Grossman et al., 2012). However, evidence was provided that proteins with molecular mass > 60 kDa, including three to four tandem fusion green fluorescent protein (GFP; c. 27 kDa for one GFP), can enter nucleus via free diffusion in vivo (Wang & Brattain, 2007; Popken

et al., 2015; Timney et al., 2016). Thus, the size exclusion limit of NPCs for free diffusion is debated (Wang & Brattain, 2007; Popken et al., 2015; Timney et al., 2016). In our model, we propose that the YFP-UVR8 monomer, c. 74 kDa, translocate into the nucleus via free diffusion. The Arabidopsis UVR8 homodimer is c. 94 kDa, which may not enter the nucleus via free diffusion within the timescale of FRAP assays. Moreover, the shape of the UVR8 homodimer may hinder its nuclear translocation. Fusing a triple YFP tag to UVR8 prevented its UV-B-induced nuclear translocation and nuclear accumulation. Moreover, adding a strong NLS to YFP-YFP-YFP-UVR8 rescued its nuclear localization and function in UV-B signaling. Overall, these observations favor the model that UVR8 monomers translocate into the nucleus via free diffusion. However, the possibility that fusion of the triple YFP tag disrupted the interaction of UVR8 with unknown nuclear import components cannot be excluded.

Because UVR8 interacts with the E3 ligase COP1 under UV-B, it can be postulated that COP1 may regulate the stability of UVR8. However, UVR8 protein levels are altered neither by UV-B (Kaiserli & Jenkins, 2007; Heijde & Ulm, 2013; Heilmann & Jenkins, 2013) nor by COP1 (Fig. S5a; Oravecz et al., 2006; Yin et al., 2016). Structural work revealed that the UV-B-activated UVR8 monomer binds to the WD40 domain of COP1 with a well-conserved VP motif, leading to COP1 inactivation (Lau et al., 2019). The blue light photoreceptor CRY2 inactivates COP1 with a similar mechanism (Ponnu et al., 2019). Therefore, the protein degradation model proposed in the introduction part is not supported by available evidence.

Using the Arabidopsis cop1-4 mutant line harboring YFP-NLS-COP1 or YFP-NES-COP1, we demonstrate that COP1 in the nucleus, but not in the cytosol, promotes UV-B-induced nuclear accumulation of UVR8. Intriguingly, we detected UV-B-induced UVR8–COP1 interaction in cytosol in the WT (Yin et al., 2016) and also in the YFP-NES-COP1 Arabidopsis line (Fig. 3f). The physiological function of the cytosolic UVR8–COP1 interaction remains unclear. Notably, UV-B induces UVR8 interaction with both YFP-NES-COP1 and YFP-NLS-COP1, yet only the latter leads to elevated nuclear UVR8 levels (Fig. 3b). These YFP-NES-COP1 lines can serve as valuable tools for further analysis of the function of cytosolic UVR8–COP1 interaction and the cytosolic activities of COP1. We propose that in the nucleus, COP1 binds to UVR8 monomer under UV-B treatment and promotes the nuclear retention of UVR8 (Fig. 5f). This retention model is further supported by the observation that UV-B also induces the colocalization and interaction of UVR8 with COP1 in the nucleus (Oravecz et al., 2006; Favory et al., 2009). The constitutively partially monomeric UVR8 mutant protein UVR8^{W285A} interacted with COP1 constitutively and localized to the nucleus at high levels in Arabidopsis irrespective of UV-B supplementation (Yin et al., 2016). The constitutively monomeric UVR8^{G101S} mutant has residual interaction with COP1 in the absence of UV-B, which is accompanied by slightly higher accumulation of its protein in the nucleus than in the WT (Fig. S7; Podolec et al., 2021b). Ultraviolet-B radiation-induces its interaction with COP1 and increases its nuclear accumulation in a COP1-dependent manner (Fig. S7; Podolec et al., 2021b). The data obtained with the UVR8

mutant variants are consistent with the COP1-dependent UVR8 nuclear retention model. In addition to COP1, several other nuclear proteins interact with UVR8 (Liang *et al.*, 2018; Yang *et al.*, 2018, 2020; Qian *et al.*, 2020). It is not known whether these proteins regulate UVR8 nuclear localization dynamics.

After UV-B treatment is terminated, nuclear UVR8 levels gradually decline. Supporting the nuclear retention model, nuclear UVR8 level is positively correlated with that of the UV-B-induced UVR8–COP1 interaction and its attenuation following UV-B treatment in wildtype. RUP1 and RUP2 are key negative regulators of the UVR8 pathway in Arabidopsis (Gruber *et al.*, 2010). A comparison of nuclear UVR8 levels and the UVR8–COP1 interaction in *rup1 rup2* and WT plants indicated that RUP1 and RUP2 inhibit the nuclear retention of UVR8 by inhibiting the UVR8–COP1 interaction (Fig. 5f). UVR8 interacts with the WD40 domain of COP1 (Favory *et al.*, 2009; Rizzini *et al.*, 2011). A recent work indicated that the structure of the COP1^{WD40} domain is similar to that of RUP2 (Wang *et al.*, 2022). Surprisingly, both RUP2 and COP1 interact with UVR8 with similar interacting surface via similar key amino acid residues (Wang *et al.*, 2022). *In vitro*, RUP2 can successfully outcompete COP1-SPA4 from UVR8 interaction (Wang *et al.*, 2022), which supports the proposed function of RUP proteins in the regulation of UVR8–COP1 interaction and UVR8 nuclear retention in this work. UV-B could not induce UVR8 nuclear accumulation in *cop1-4 rup1 rup2* and UVR8 can exit the nucleus in the *rup1 rup2* mutant background as revealed by FLIP assays, suggesting that RUP1 and RUP2 are not essential for UVR8 nuclear exit. RUP1 and RUP2 previously were shown to inhibit UV-B signaling by accelerating the re-binding of UVR8 monomers to form inactive homodimers (Heijde & Ulm, 2013). In another study, RUP1 and RUP2 were shown to act in an E3 ligase complex targeting HY5 for degradation to negatively regulate UV-B signaling (Ren *et al.*, 2019). Here we show that RUP1 and RUP2 also can inactivate UV-B signaling via inhibiting UVR8 nuclear retention. Thus, RUP1 and RUP2 may inhibit UV-B signaling via distinct mechanisms. Currently, it is not clear how COP1 binding promotes UVR8 nuclear retention. It is plausible that the relatively large molecular mass of UVR8/COP1 heterodimer (*c.* 122 kDa) may slow down its nuclear exit. Moreover, UVR8–COP1 interaction may block the NES of COP1 to promote UVR8 nuclear accumulation. It also is possible that binding of COP1 blocks the binding of an unknown NES-containing protein to UVR8.

In summary, we propose that UV-B-induced monomerization of UVR8 and the concurrent size reduction promotes UVR8 nuclear translocation via diffusion. In the nucleus, COP1 binding promotes UVR8 nuclear retention, which is counterbalanced by RUP1 and RUP2. A COP1-independent co-import of UVR8 into the nucleus under UV-B is possible, a hypothesis which awaits further investigations.

Acknowledgements

Author contributions

RY and RU designed the research; FF, LL, Qianwen Zhang, MYS, RP, Qinyun Zhang, JP, CZ and RY performed research; FF, LL, ML and RY analyzed data; and FF, LL, RU and RY wrote the paper. FF, LL and Qianwen Zhang contributed equally to this work.

ORCID

Fang Fang https://orcid.org/0000-0001-6595-4102
Li Lin https://orcid.org/0000-0003-3219-6020
Jiahao Pi https://orcid.org/0000-0002-0380-3699
Roman Podolec https://orcid.org/0000-0003-2998-7892
Roman Ulm https://orcid.org/0000-0001-8014-7392
Ruohe Yin https://orcid.org/0000-0001-6782-4651
Chunli Zhang https://orcid.org/0000-0003-2431-607X
Qianwen Zhang https://orcid.org/0000-0002-0646-3415
Qinyun Zhang https://orcid.org/0000-0001-6758-5646

Data availability

The data that supports the findings of this study are available in the Supporting Information of this article.

References

von Arnim AG, Deng XW. 1994. Light inactivation of Arabidopsis photomorphogenic repressor COP1 involves a cell-specific regulation of its nucleocytoplasmic partitioning. *Cell* 79: 1035–1045.

Brown BA, Cloix C, Jiang GH, Kaiserli E, Herzyk P, Kliebenstein DJ, Jenkins GI. 2005. A UV-B-specific signaling component orchestrates plant UV protection. *Proceedings of the National Academy of Sciences, USA* 102: 18225–18230.

Brown BA, Jenkins GI. 2008. UV-B signaling pathways with different fluence-rate response profiles are distinguished in mature Arabidopsis leaf tissue by requirement for UVR8, HY5, and HYH. *Plant Physiology* 146: 576–588.

Chen M, Tao Y, Lim J, Shaw A, Chory J. 2005. Regulation of phytochrome B nuclear localization through light-dependent unmasking of nuclear-localization signals. *Current Biology* 15: 637–642.

Christie JM, Arvai AS, Baxter KJ, Heilmann M, Pratt AJ, O'Hara A, Kelly SM, Hothorn M, Smith BO, Hitomi K *et al.* 2012. Plant UVR8 photoreceptor senses UV-B by tryptophan-mediated disruption of cross-dimer salt bridges. *Science* 335: 1492–1496.

Cloix C, Kaiserli E, Heilmann M, Baxter KJ, Brown BA, O'Hara A, Smith BO, Christie JM, Jenkins GI. 2012. C-terminal region of the UV-B photoreceptor UVR8 initiates signaling through interaction with the COP1 protein. *Proceedings of the National Academy of Sciences, USA* 109: 16366–16370.

Crefcoeur RP, Yin R, Ulm R, Halazonetis TD. 2013. Ultraviolet-B-mediated induction of protein-protein interactions in mammalian cells. *Nature Communications* 4: 1779.

Favory JJ, Stec A, Gruber H, Rizzini L, Oravecz A, Funk M, Albert A, Cloix C, Jenkins GI, Oakeley EJ *et al.* **2009.** Interaction of COP1 and UVR8 regulates UV-B-induced photomorphogenesis and stress acclimation in Arabidopsis. *EMBO Journal* **28**: 591–601.

Findlay KM, Jenkins GI. **2016.** Regulation of UVR8 photoreceptor dimer/monomer photo-equilibrium in Arabidopsis plants grown under photoperiodic conditions. *Plant, Cell & Environment* **39**: 1706–1714.

Galvao VC, Fankhauser C. **2015.** Sensing the light environment in plants: photoreceptors and early signaling steps. *Current Opinion in Neurobiology* **34**: 46–53.

Genoud T, Schweizer F, Tscheuschler A, Debrieux D, Casal JJ, Schafer E, Hiltbrunner A, Fankhauser C. **2008.** FHY1 mediates nuclear import of the light-activated phytochrome A photoreceptor. *PLoS Genetics* **4**: e1000143.

Grossman E, Medalia O, Zwerger M. **2012.** Functional architecture of the nuclear pore complex. *Annual Review of Biophysics* **41**: 557–584.

Gruber H, Heijde M, Heller W, Albert A, Seidlitz HK, Ulm R. **2010.** Negative feedback regulation of UV-B-induced photomorphogenesis and stress acclimation in Arabidopsis. *Proceedings of the National Academy of Sciences, USA* **107**: 20132–20137.

Han X, Chang X, Zhang Z, Chen H, He H, Zhong B, Deng XW. **2019.** Origin and evolution of core components responsible for monitoring light environment changes during plant terrestrialization. *Molecular Plant* **12**: 847–862.

Heijde M, Binkert M, Yin R, Ares-Orpel F, Rizzini L, Van De Slijke E, Persiau G, Nolf J, Gevaert K, De Jaeger G *et al.* **2013.** Constitutively active UVR8 photoreceptor variant in Arabidopsis. *Proceedings of the National Academy of Sciences, USA* **110**: 20326–20331.

Heijde M, Ulm R. **2013.** Reversion of the Arabidopsis UV-B photoreceptor UVR8 to the homodimeric ground state. *Proceedings of the National Academy of Sciences, USA* **110**: 1113–1118.

Heilmann M, Jenkins GI. **2013.** Rapid reversion from monomer to dimer regenerates the ultraviolet-B photoreceptor UV RESISTANCE LOCUS8 in intact Arabidopsis plants. *Plant Physiology* **161**: 547–555.

Hiltbrunner A, Viczian A, Bury E, Tscheuschler A, Kircher S, Toth R, Honsberger A, Nagy F, Fankhauser C, Schafer E. **2005.** Nuclear accumulation of the phytochrome A photoreceptor requires FHY1. *Current Biology* **15**: 2125–2130.

Huang X, Yang P, Ouyang X, Chen L, Deng XW. **2014.** Photoactivated UVR8-COP1 module determines photomorphogenic UV-B signaling output in Arabidopsis. *PLoS Genetics* **10**: e1004218.

Jenkins GI. **2017.** Photomorphogenic responses to ultraviolet-B light. *Plant, Cell & Environment* **40**: 2544–2557.

Kaiserli E, Jenkins GI. **2007.** UV-B promotes rapid nuclear translocation of the Arabidopsis UV-B specific signaling component UVR8 and activates its function in the nucleus. *Plant Cell* **19**: 2662–2673.

Karimi M, Inze D, Depicker A. **2002.** GATEWAY vectors for *Agrobacterium*-mediated plant transformation. *Trends in Plant Science* **7**: 193–195.

Kinkema M, Fan W, Dong X. **2000.** Nuclear localization of NPR1 is required for activation of PR gene expression. *Plant Cell* **12**: 2339–2350.

Kliebenstein DJ, Lim JE, Landry LG, Last RL. **2002.** Arabidopsis UVR8 regulates ultraviolet-B signal transduction and tolerance and contains sequence similarity to human regulator of chromatin condensation 1. *Plant Physiology* **130**: 234–243.

Klose C, Viczian A, Kircher S, Schafer E, Nagy F. **2015.** Molecular mechanisms for mediating light-dependent nucleo/cytoplasmic partitioning of phytochrome photoreceptors. *The New Phytologist* **206**: 965–971.

Kong SG, Suzuki T, Tamura K, Mochizuki N, Hara-Nishimura I, Nagatani A. **2006.** Blue light-induced association of phototropin 2 with the Golgi apparatus. *The Plant Journal* **45**: 994–1005.

Lau K, Podolec R, Chappuis R, Ulm R, Hothorn M. **2019.** Plant photoreceptors and their signaling components compete for COP1 binding via VP peptide motifs. *EMBO Journal* **38**: e102140.

Li X, Liu Z, Ren H, Kundu M, Zhong FW, Wang L, Gao J, Zhong D. **2022.** Dynamics and mechanism of dimer dissociation of photoreceptor UVR8. *Nature Communications* **13**: 93.

Liang T, Mei S, Shi C, Yang Y, Peng Y, Ma L, Wang F, Li X, Huang X, Yin Y *et al.* **2018.** UVR8 interacts with BES1 and BIM1 to regulate transcription and photomorphogenesis in Arabidopsis. *Developmental Cell* **44**: 512–523 e515.

Liang T, Yang Y, Liu H. **2019.** Signal transduction mediated by the plant UV-B photoreceptor UVR8. *The New Phytologist* **221**: 1247–1252.

Lin L, Dong H, Yang G, Yin R. **2020.** The C-terminal 17 amino acids of the photoreceptor UVR8 is involved in the fine-tuning of UV-B signaling. *Journal of Integrative Plant Biology* **62**: 1327–1340.

Liu X, Zhang Q, Yang G, Zhang C, Dong H, Liu Y, Yin R, Lin L. **2020.** Pivotal roles of tomato photoreceptor SlUVR8 in seedling development and UV-B stress tolerance. *Biochemical and Biophysical Research Communications* **522**: 177–183.

McNellis TW, von Arnim AG, Araki T, Komeda Y, Misera S, Deng XW. **1994.** Genetic and molecular analysis of an allelic series of cop1 mutants suggests functional roles for the multiple protein domains. *Plant Cell* **6**: 487–500.

O'Hara A, Jenkins GI. **2012.** *In vivo* function of tryptophans in the Arabidopsis UV-B photoreceptor UVR8. *Plant Cell* **24**: 3755–3766.

Oravecz A, Baumann A, Mate Z, Brzezinska A, Molinier J, Oakeley EJ, Adam E, Schafer E, Nagy F, Ulm R. **2006.** CONSTITUTIVELY PHOTOMORPHOGENIC1 is required for the UV-B response in Arabidopsis. *Plant Cell* **18**: 1975–1990.

Ordonez-Herrera N, Fackendahl P, Yu X, Schaefer S, Koncz C, Hoecker U. **2015.** A cop1 spa mutant deficient in COP1 and SPA proteins reveals partial co-action of COP1 and SPA during Arabidopsis post-embryonic development and photomorphogenesis. *Molecular Plant* **8**: 479–481.

Pfeiffer A, Nagel MK, Popp C, Wust F, Bindics J, Viczian A, Hiltbrunner A, Nagy F, Kunkel T, Schafer E. **2012.** Interaction with plant transcription factors can mediate nuclear import of phytochrome B. *Proceedings of the National Academy of Sciences, USA* **109**: 5892–5897.

Podolec R, Demarsy E, Ulm R. **2021a.** Perception and signaling of ultraviolet-B radiation in plants. *Annual Review of Plant Biology* **72**: 793–822.

Podolec R, Lau K, Wagnon TB, Hothorn M, Ulm R. **2021b.** A constitutively monomeric UVR8 photoreceptor confers enhanced UV-B photomorphogenesis. *Proceedings of the National Academy of Sciences, USA* **118**: e20172841.

Podolec R, Wagnon TB, Leonardelli M, Johansson H, Ulm R. **2022.** Arabidopsis B-box transcription factors BBX20-22 promote UVR8 photoreceptor-mediated UV-B responses. *The Plant Journal* **111**: 422–439.

Ponnu J, Riedel T, Penner E, Schrader A, Hoecker U. **2019.** Cryptochrome 2 competes with COP1 substrates to repress COP1 ubiquitin ligase activity during Arabidopsis photomorphogenesis. *Proceedings of the National Academy of Sciences, USA* **116**: 27133–27141.

Popken P, Ghavami A, Onck PR, Poolman B, Veenhoff LM. **2015.** Size-dependent leak of soluble and membrane proteins through the yeast nuclear pore complex. *Molecular Biology of the Cell* **26**: 1386–1394.

Qian C, Chen Z, Liu Q, Mao W, Chen Y, Tian W, Liu Y, Han J, Ouyang X, Huang X. **2020.** Coordinated transcriptional regulation by the UV-B photoreceptor and multiple transcription factors for plant UV-B responses. *Molecular Plant* **13**: 777–792.

Qian C, Mao W, Liu Y, Ren H, Lau OS, Ouyang X, Huang X. **2016.** Dual-source nuclear monomers of UV-B light receptor direct photomorphogenesis in Arabidopsis. *Molecular Plant* **9**: 1671–1674.

Qin N, Xu D, Li J, Deng XW. **2020.** COP9 signalosome: discovery, conservation, activity, and function. *Journal of Integrative Plant Biology* **62**: 90–103.

Rai N, Neugart S, Yan Y, Wang F, Siipola SM, Lindfors AV, Winkler JB, Albert A, Brosche M, Lehto T *et al.* **2019.** How do cryptochromes and UVR8 interact in natural and simulated sunlight? *Journal of Experimental Botany* **70**: 4975–4990.

Rausenberger J, Tscheuschler A, Nordmeier W, Wust F, Timmer J, Schafer E, Fleck C, Hiltbrunner A. **2011.** Photoconversion and nuclear trafficking cycles determine phytochrome A's response profile to far-red light. *Cell* **146**: 813–825.

Ren H, Han J, Yang P, Mao W, Liu X, Qiu L, Qian C, Liu Y, Chen Z, Ouyang X *et al.* **2019.** Two E3 ligases antagonistically regulate the UV-B response in Arabidopsis. *Proceedings of the National Academy of Sciences, USA* **116**: 4722–4731.

Rizzini L, Favory JJ, Cloix C, Faggionato D, O'Hara A, Kaiserli E, Baumeister R, Schafer E, Nagy F, Jenkins GI *et al.* **2011.** Perception of UV-B by the Arabidopsis UVR8 protein. *Science* **332**: 103–106.

Ronald J, Davis SJ. **2019.** Focusing on the nuclear and subnuclear dynamics of light and circadian signalling. *Plant, Cell & Environment* **42**: 2871–2884.

Sakamoto K, Briggs WR. 2002. Cellular and subcellular localization of phototropin 1. *Plant Cell* 14: 1723–1735.

Sharma A, Sharma B, Hayes S, Kerner K, Hoecker U, Jenkins GI, Franklin KA. 2019. UVR8 disrupts stabilisation of PIF5 by COP1 to inhibit plant stem elongation in sunlight. *Nature Communications* 10: 4417.

Shi C, Liu H. 2021. How plants protect themselves from ultraviolet-B radiation stress. *Plant Physiology* 187: 1096–1103.

Stacey MG, Hicks SN, von Arnim AG. 1999. Discrete domains mediate the light-responsive nuclear and cytoplasmic localization of Arabidopsis COP1. *Plant Cell* 11: 349–364.

Tada Y, Spoel SH, Pajerowska-Mukhtar K, Mou Z, Song J, Wang C, Zuo J, Dong X. 2008. Plant immunity requires conformational changes (corrected) of NPR1 via S-nitrosylation and thioredoxins. *Science* 321: 952–956.

Tavridou E, Pireyre M, Ulm R. 2020a. Degradation of the transcription factors PIF4 and PIF5 under UV-B promotes UVR8-mediated inhibition of hypocotyl growth in Arabidopsis. *The Plant Journal* 101: 507–517.

Tavridou E, Schmid-Siegert E, Fankhauser C, Ulm R. 2020b. UVR8-mediated inhibition of shade avoidance involves HFR1 stabilization in Arabidopsis. *PLoS Genetics* 16: e1008797.

Timney BL, Raveh B, Mironska R, Trivedi JM, Kim SJ, Russel D, Wente SR, Sali A, Rout MP. 2016. Simple rules for passive diffusion through the nuclear pore complex. *The Journal of Cell Biology* 215: 57–76.

Tissot N, Ulm R. 2020. Cryptochrome-mediated blue-light signalling modulates UVR8 photoreceptor activity and contributes to UV-B tolerance in Arabidopsis. *Nature Communications* 11: 1323.

Ulm R, Baumann A, Oravecz A, Mate Z, Adam E, Oakeley EJ, Schafer E, Nagy F. 2004. Genome-wide analysis of gene expression reveals function of the bZIP transcription factor HY5 in the UV-B response of Arabidopsis. *Proceedings of the National Academy of Sciences, USA* 101: 1397–1402.

Wang R, Brattain MG. 2007. The maximal size of protein to diffuse through the nuclear pore is larger than 60kDa. *FEBS Letters* 581: 3164–3170.

Wang Y, Wang L, Guan Z, Chang H, Ma L, Shen C, Qiu L, Yan J, Zhang D, Li J *et al.* 2022. Structural insight into UV-B-activated UVR8 bound to COP1. *Science Advances* 8: eabn3337.

Wu D, Hu Q, Yan Z, Chen W, Yan C, Huang X, Zhang J, Yang P, Deng H, Wang J *et al.* 2012. Structural basis of ultraviolet-B perception by UVR8. *Nature* 484: 214–219.

Wu Y, Zhang D, Chu JY, Boyle P, Wang Y, Brindle ID, De Luca V, Despres C. 2012. The Arabidopsis NPR1 protein is a receptor for the plant defense hormone salicylic acid. *Cell Reports* 1: 639–647.

Yang G, Zhang C, Dong H, Liu X, Guo H, Tong B, Fang F, Zhao Y, Yu Y, Liu Y *et al.* 2022. Activation and negative feedback regulation of SlHY5 transcription by the SlBBX20/21-SlHY5 transcription factor module in UV-B signaling. *Plant Cell* 34: 2038–2055.

Yang Y, Liang T, Zhang L, Shao K, Gu X, Shang R, Shi N, Li X, Zhang P, Liu H. 2018. UVR8 interacts with WRKY36 to regulate HY5 transcription and hypocotyl elongation in Arabidopsis. *Nature Plants* 4: 98–107.

Yang Y, Zhang L, Chen P, Liang T, Li X, Liu H. 2020. UV-B photoreceptor UVR8 interacts with MYB73/MYB77 to regulate auxin responses and lateral root development. *EMBO Journal* 39: e101928.

Yi C, Deng XW. 2005. COP1 - from plant photomorphogenesis to mammalian tumorigenesis. *Trends in Cell Biology* 15: 618–625.

Yin R, Arongaus AB, Binkert M, Ulm R. 2015. Two distinct domains of the UVR8 photoreceptor interact with COP1 to initiate UV-B signaling in Arabidopsis. *Plant Cell* 27: 202–213.

Yin R, Skvortsova MY, Loubery S, Ulm R. 2016. COP1 is required for UV-B-induced nuclear accumulation of the UVR8 photoreceptor. *Proceedings of the National Academy of Sciences, USA* 113: E4415–E4422.

Yin R, Ulm R. 2017. How plants cope with UV-B: from perception to response. *Current Opinion in Plant Biology* 37: 42–48.

Zhang CL, Zhang QW, Guo HY, Yu XH, Liang WJ, Chen YH, Yin RH, Lin L. 2021. Tomato SlRUP is a negative regulator of UV-B photomorphogenesis. *Molecular Horticulture* 1: 1–4.

Supporting Information

Additional Supporting Information may be found online in the Supporting Information section at the end of the article.

Fig. S1 Sequence of synthetic yellow fluorescent protein (YFP)-YFP-UV RESISTANCE LOCUS 8 (UVR8) and NLS-YFP-YFP-UVR8.

Fig. S2 No nuclear translocation of yellow fluorescent protein-HY5 fusion protein was observed with fluorescence recovery after photobleaching assays.

Fig. S3 Corresponding to Fig. 1b (the same blot was used in Figs 1b, S3; the *uvr8-6* mutant is included in Fig. S3).

Fig. S4 Yellow fluorescent protein (YFP)-YFP-YFP-UV RESISTANCE LOCUS 8 (UVR8) fusion proteins form homodimers and respond to ultraviolet-B radiation similar to UVR8.

Fig. S5 Immunoblotting analysis of yellow fluorescent protein-CONSTITUTIVELY PHOTOMORPHOGENIC 1 and UV RESISTANCE LOCUS 8 proteins.

Fig. S6 SlRUP inhibits ultraviolet-B radiation-induced SlUVR8 nuclear accumulation.

Fig. S7 Immunoblot analysis of UV RESISTANCE LOCUS 8, UGPase (cytosolic marker) and H3 (nuclear marker) levels in cytosolic and nuclear extracts.

Table S1 Primers used in this work.

Please note: Wiley Blackwell are not responsible for the content or functionality of any Supporting Information supplied by the authors. Any queries (other than missing material) should be directed to the *New Phytologist* Central Office.